Advances in Science and Technology Research Journal

Advances in Science and Technology Research Journal, 2026, 20(6), 473–487
https://doi.org/10.12913/22998624/218992
ISSN 2299-8624, License CC-BY 4.0

Received: 2026.02.15
Accepted: 2026.04.15
Published: 2026.05.01

The influence of bond stress on crack formation and development in lightweight aggregate reinforced concrete

Vu Dinh Tho[1], Ngoc Lan Le[1*], Hung Phong Nguyen[2], Hien Pham Thi[1]

[1] Department of Civil and Industrial Construction, Faculty of Civil Engineering, University of Transport Technology, 54 Trieu Khuc Street, Thanh Xuan District, Hanoi, 100000, Vietnam
[2] Faculty of Building and Industrial Construction, Hanoi University of Civil Engineering, Vietnam
* Corresponding author's e-mail: lanln@utt.edu.vn

ABSTRACT

This paper presents the results of both theoretical and experimental studies on the influence of bond stress on the formation and development of cracks in reinforced concrete beams made with 100% recycled lightweight aggregates. Experimental studies to determine the parameters of concrete using recycled lightweight aggregate (RLWA) were carried out on three mix designs, M1, M2, and M3, with corresponding compressive strengths of 15 MPa, 25 MPa, and 35 MPa, respectively. The experiments to determine the bond-slip relationship between recycled lightweight aggregate concrete and reinforcing steel were conducted on cubic specimens with dimensions of 150 × 150 × 150 mm and reinforcing bars with a diameter of d = 12 mm The tests investigating the cracking behavior of reinforced beams made of recycled lightweight aggregate concrete (RLWAC) under flexural loading were carried out on beam specimens under four – point loading with simply supported supports. The cracking moment, the cracking width at steel yield, and the cracking width at the maximum moment of the beams were compared with the provisions of TCVN 5574-2018 and Eurocode 2 and the proposed theoretical method. The research results indicate that the bond strength between reinforcing steel and recycled lightweight aggregate concrete is lower than that of conventional concrete. This is mainly attributed to the weak interfacial transition zone (ITZ), the porous nature, and the high water absorption of the recycled lightweight aggregates. The results from tests on reinforced concrete beams under flexure showed that RLWAC beams exhibited earlier crack initiation, faster crack propagation, and larger crack widths than conventional reinforced concrete beams. The analytical results based on the proposed theoretical model for calculating the cracking moment and crack width of reinforced concrete beams using RLWAC are closer to the experimental results (with errors of 2–7% for cracking moment and 19–23% for crack width) than those obtained according to TCVN 5574:2018 and Eurocode 2. These results contribute to establishing a scientific basis for the design and crack control of reinforced concrete members using RLWAC.

Keywords: recycled lightweight aggregate, recycled lightweight aggregate concrete, bond stress, Bond–slip relationship, crack initiation and propagation, reinforced concrete beam.

INTRODUCTION

In recent years, the amount of construction waste generated from the demolition and renovation of buildings has increased significantly, placing great pressure on the urban environment and waste management systems. Recycling construction waste to produce recycled aggregates is considered a suitable approach in line with the sustainable development strategies and circular economy in the construction sector. Therefore, many researchers have investigated the use of recycled materials in concrete production such as: studies on the mechanical properties of concrete incorporating recycled aggregate have been reported in [1, 2]; research on the quality of coarse aggregate mixture can be found in [3, 4]; investigated on the strength and shrinkage of concrete mixtures presented in [5, 6]. Lightweight concrete using recycled lightweight aggregate offers advantages in reducing self-weight, improving thermal insulation, and utilizing construction

waste materials [7, 8]. However, the mechanical properties of RLWAC differ significantly from those of conventional normal-weight concrete (BTT). This difference mainly stems from the characteristics of recycled lightweight aggregate particles, which typically exhibit a porous structure, high water absorption, and relatively low compressive strength of recycled aggregate [9, 10]. In the study of the authors [11, 12] the influence of the bond behavior between reinforcing steel and RLWAC was investigated.

The research results of the above authors have shown that the bond stress between the steel reinforcement and concrete. These studies have shown that the bond stress between the steel reinforcement and the concrete governs the transfer of force from the reinforcement to the concrete and vice versa. This is an important factor determining the simultaneous working of reinforced concrete structures under loading. In publications [13] research on the influence of different types of recycled lightweight aggregate concrete on the bonding behavior between steel reinforcement and concrete. Several studies [14, 15] have been conducted to consider the influence of different parameters (such as the replacement rate of recycled lightweight aggregate, the water-to-cement ratio, type and diameter of steel reinforcement, and the position of reinforcement) on the bond strength of steel reinforcement in recycled lightweight aggregate concrete. Most studies [16] have shown that RLWAC generally exhibits lower bond strength to steel reinforcement than conventional concrete. However, some types of recycled aggregate concrete reported in [17] have shown bond strength between steel and RLWAC comparable to or even higher than that of normal reinforced concrete.

Weak bond strength can lead to premature cracking, increased relative slip between reinforcement and concrete, thereby affecting load transfer and promoting crack widening in the tensile zone of the concrete. Therefore, a thorough understanding of the bond strength characteristics of RLWAC is essential for accurately describing the cracking behavior of the structural members.

Although many studies have been conducted worldwide on lightweight concrete and recycled concrete, the number of studies that thoroughly investigate the relationship between bond stress and the mechanisms of crack initiation and propagation in reinforced concrete beams using recycled lightweight aggregate remains limited. Current design standards, such as TCVN 5574:2018 [18] and Eurocode 2 [19], which were developed for conventional normal-weight concrete and traditional lightweight concrete, do not accurately reflect the mechanical properties of RLWAC. Therefore, developing separate theoretical models for this type of material is extremely necessary.

In this study, RLWA was used from the technological process of Mueller et al. [20], Three RLWAC mixes with different strength levels were tested to determine their mechanical properties and stress-strain relationship. Bond – slip tests were conducted investigate the bond stress behavior and to develop an appropriate τ–s model for this type of concrete. Finally, experiments on RLWAC beams subjected to pure bending were carried out to evaluate the cracking mechanism and to establish a theoretical model for predicting the cracking moment and crack width.

The research results clarify the relationship between bond stress and the influence of crack development in RLWAC beams, and provide a scientific basis for construction and design guidance to be more appropriate for structural members using this material.

MATERIALS AND METHODS

Materials

In this study, the concrete materials and mix design incorporated RLWA produced from construction and demolition waste following the procedure proposed by Mueller et al. (2008) [20]. The RLWA were classified into size ranges: S2 (4–8 mm) and S3 (8–16 mm) (Figure 1). The S2 coarse aggregates had a bulk density of approximately 430 kg/m³ and a water absorption of 28%, whereas the S3 aggregates had a bulk density of 369 kg/m³ and a water absorption of 32%. The crushing value test conducted in accordance with TCVN 7572-11:2006 [21] yielded values of 53.5% and 43.47% for the S2 and S3 aggregates, respectively (Figure 2). These results reflect the porous structure and the relatively low crushing strength characteristic of RLWA. In addition, Portland cement, fly ash, and a superplasticizer were used to improve workability and to ensure the target design strength of 15, 25, and 35 MPa for mixes M1, M2, and M3, respectively.

The concrete mix designs incorporating recycled aggregates consisted of three mixes: M1, M2, and M3 (Table 1). These mixes were

designed with the same water-to-binder ratio and target compressive strengths of approximately 15 MPa, 25 MPa, and 35 MPa, respectively. The dry bulk density of RLWAC, measured after 28 days of curing at room temperature, ranges from 1715 to 1775 kg/m³ In this study, the concrete materials and mix design incorporated RLWA produced from construction and demolition waste following the procedure proposed by Mueller et al. (2008) [20]. The RLWA were classified into size ranges: S2 (4–8 mm) and S3 (8–16 mm) (Figure 1). The S2 coarse aggregates had a bulk density of approximately 430 kg/m³ and a water absorption of 28%, whereas the S3 aggregates had a bulk density of 369 kg/m³ and a water absorption of 32%. The crushing value test conducted in accordance with TCVN 7572-11:2006 [21] yielded values of 53.5% and 43.47% for the S2 and S3 aggregates, respectively (Figure 2). These results reflect the porous structure and the relatively low crushing strength characteristic of RLWA. In addition, Portland cement, fly ash, and a superplasticizer were used to improve workability and to ensure the target design strength of 15, 25, and 35 MPa for mixes M1, M2, and M3, respectively.

The concrete mix designs incorporating recycled aggregates consisted of three mixes: M1, M2, and M3 (Table 1). These mixes were designed with the same water-to-binder ratio and target compressive strengths of approximately 15 MPa, 25 MPa, and 35 MPa, respectively. The dry bulk density of RLWAC, measured after 28 days of curing at room temperature, ranges from 1715 to 1775 kg/m³ In this study, the concrete materials and mix design incorporated RLWA produced from construction and demolition waste following the procedure proposed by Mueller et al. (2008) [20]. The RLWA were classified into size ranges: S2 (4–8 mm) and S3 (8–16 mm) (Figure 1). The S2 coarse aggregates had a bulk density of approximately 430 kg/m³ and a water absorption of 28%, whereas the S3 aggregates had a bulk density of 369 kg/m³ and a water absorption of 32%. The crushing value test conducted in accordance with TCVN 7572-11:2006 [21] yielded values of 53.5% and 43.47% for the S2 and S3 aggregates, respectively (Figure 2). These results reflect the porous structure and the relatively low crushing strength characteristic of RLWA. In addition, Portland cement, fly ash, and a superplasticizer were used to improve workability and to ensure the target design strength of 15, 25, and 35 MPa for mixes M1, M2, and M3, respectively.

Figure 1. Recycled coarse aggregate

The concrete mix designs incorporating recycled aggregates consisted of three mixes: M1, M2, and M3 (Table 1). These mixes were designed with the same water-to-binder ratio and target compressive strengths of approximately 15 MPa, 25 MPa, and 35 MPa, respectively. The dry bulk density of RLWAC, measured after 28 days of curing at room temperature, ranges from 1715 to 1775 kg/m³ In this study, the concrete materials and mix design incorporated RLWA produced from construction and demolition waste following the procedure proposed by Mueller et al. (2008) [20]. The RLWA were classified into size ranges: S2 (4–8 mm) and S3 (8–16 mm) (Figure 1). The S2 coarse aggregates had a bulk density of approximately 430 kg/m³ and a water absorption of 28%, whereas the S3 aggregates had a bulk density of 369 kg/m³ and a water absorption of 32%. The crushing value test conducted in accordance with TCVN 7572-11:2006 [21] yielded values of 53.5% and 43.47% for the S2 and S3 aggregates, respectively (Figure 2). These results reflect the porous structure and the relatively low crushing strength characteristic of RLWA. In addition, Portland cement, fly ash, and a superplasticizer were used to improve workability and to ensure the target design strength of 15, 25, and 35 MPa for mixes M1, M2, and M3, respectively.

The concrete mix designs incorporating recycled aggregates consisted of three mixes: M1, M2, and M3 (Table 1). These mixes were designed with the same water-to-binder ratio and target compressive strengths of approximately 15 MPa, 25 MPa, and 35 MPa, respectively. The dry bulk density of RLWAC, measured after 28 days of curing at room temperature, ranges from 1715 to 1775 kg/m³ In this study, the concrete materials and mix design incorporated RLWA produced from construction and demolition

Figure 2. S2 and S3 aggregate samples after the crushing test and sieving through different sieve sizes

waste following the procedure proposed by Mueller et al. (2008) [20]. The RLWA were classified into size ranges: S2 (4–8 mm) and S3 (8–16 mm) (Figure 1). The S2 coarse aggregates had a bulk density of approximately 430 kg/m³ and a water absorption of 28%, whereas the S3 aggregates had a bulk density of 369 kg/m³ and a water absorption of 32%. The crushing value test conducted in accordance with TCVN 7572-11:2006 [21] yielded values of 53.5% and 43.47% for the S2 and S3 aggregates, respectively (Figure 2). These results reflect the porous structure and the relatively low crushing strength characteristic of RLWA. In addition, Portland cement, fly ash, and a superplasticizer were used to improve workability and to ensure the target design strength of 15, 25, and 35 MPa for mixes M1, M2, and M3, respectively.

The concrete mix designs incorporating recycled aggregates consisted of three mixes: M1, M2, and M3 (Table 1). These mixes were designed with the same water-to-binder ratio and target compressive strengths of approximately 15 MPa, 25 MPa, and 35 MPa, respectively. The dry bulk density of RLWAC, measured after 28 days of curing at room temperature, ranges from 1715 to 1775 kg/m³

Mechanical properties

Compressive strength was determined on 150 × 300 mm cylindrical specimens in accordance with TCVN 3118:2022 [22]; flexural tensile strength on 100 × 100 × 400 mm prismatic specimens according to TCVN 3119:2022 [23]; and splitting tensile strength on 150 × 300 mm cylindrical specimens in accordance with TCVN 8862:2011 [24]. For each test, 9 specimens were prepared, corresponding to the 3 mix designs M1, M2, and M3.

The elastic modulus and stress-strain relationship under compression were determined in accordance with ASTM C469 [25] using 150 × 300 mm cylindrical specimens. For each mix, 6 specimens were used to measure the elastic modulus, and 3 specimens were tested to failure.

The axial compressive strain of the concrete specimens was measured using electrical resistance strain gauges attached to the concrete surface during the loading process. The experimental results provided the mechanical properties of RLWAC, including compressive strength, tensile strength, elastic modulus, and the stress-strain relationship (Figure 3). These parameters were used as inputs for subsequent analyses of bond stress and the mechanisms of crack initiation and propagation in reinforced concrete beams.

Table 1. Concrete mix design and bulk density of recycled lightweight aggregate concrete

ID	W/B	V_{RA}/Vc	Vs/V_{RA}	FA/B (%)	SP/B (%)	Fresh density (kg/m³)	Coefficient of variation	Dry density, ρ_c (kg/m³)	Coefficient of variation
M3	0.36	0.35	0.45	27.61%	1%	1798	0.012	1775	0.016
M2	0.36	0.31	0.45	27.61%	1%	1783	0.011	1762	0.019
M1	0.36	0.28	0.45	27.61%	1%	1773	0.023	1715	0.047

Note: + W/B is the water-to-binder ratio, + V_{RA}/V_c is the ratio of recycled coarse aggregate to concrete (by volume), + Vs/V_{RA} is the ratio of sand to recycled coarse aggregate (by volume), + FA/B is the ratio of fly ash to the mass of binder, + SP/B is the ratio of superplasticizer to the mass of binder.

Bond stress test

The bond stress between steel reinforcement and RLWAC was determined using the test method proposed by RILEM and SNIP 2.03.01-84 [26]. For each mix (M1, M2, and M3), 3 cubic specimens with dimensions of 150 × 150 × 150 mm were prepared. The reinforcing bars used were CB400V steel with a nominal diameter of 12 mm, placed at the center of the specimens, as shown in Figure 4. The length of the steel reinforcement embedded in the concrete was taken as 5d (60 mm). The pull-out load was gradually applied to the steel reinforcement bars until the steel slipped out of the concrete. The relative slip of the steel bar with respect to the concrete was measured directly during loading. From the experimental results, the characteristic bond parameters, including maximum bond stress, corresponding slip at the maximum state, and residual bond stress, were determined, serving for the analysis of the cracking mechanism and modeling of the behavior of reinforced concrete beams in the following sections.

Flexural test

The flexural behavior test of reinforced concrete beams using RLWA was conducted on beam specimens with a cross-section of 150 × 200 mm and a span of 2000 mm. The experimental setup and applied loads are shown in Figure 5 and Table 2. The beam was loaded with two concentrated loads spaced 400 mm apart (twice the beam height) located in the middle of the beam, creating a purely bending section.

The concrete materials used are M1, M2, and M3 mixes as shown in Table 1. The reinforcement steel used is CB400V, with the specifications shown in Table 3

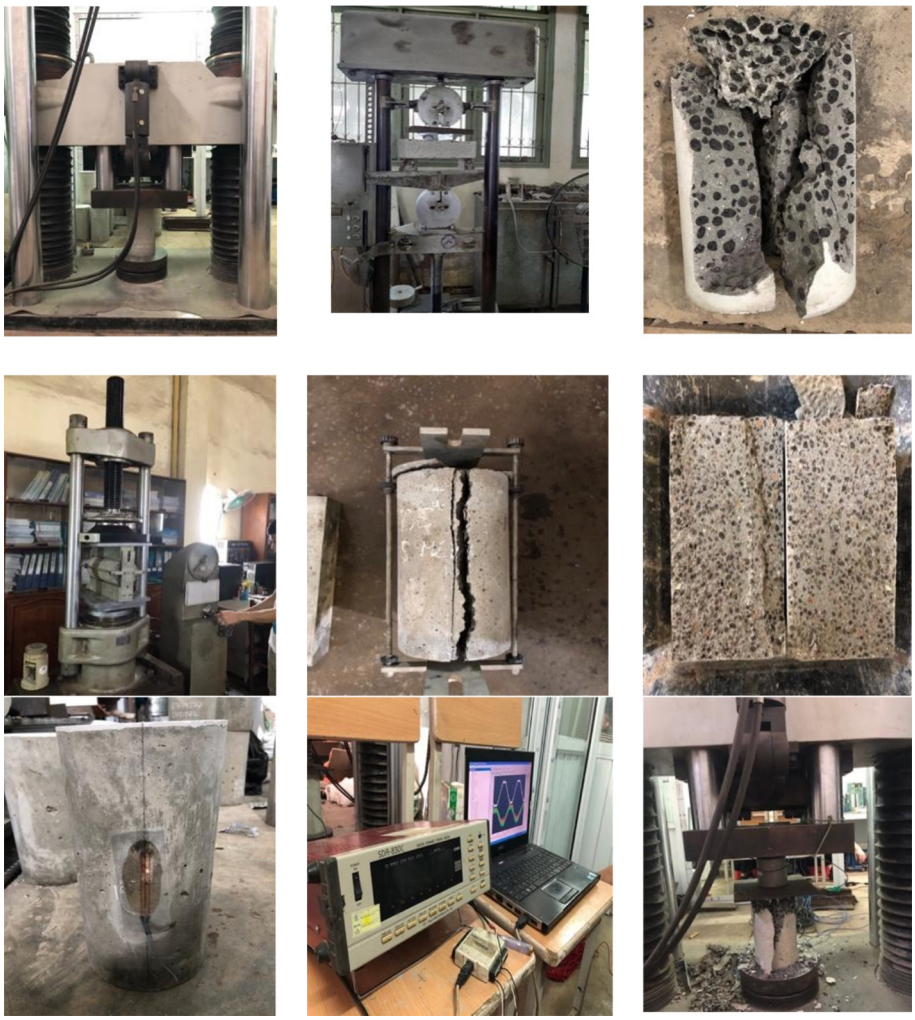

Figure 3. Test specimens, testing equipment, and failed specimens from the mechanical and physical property tests of recycled lightweight aggregate concrete

Figure 4. Test specimens, pull-out test setup, and failed specimens

Table 2. Characteristic parameters of the experimental beams

STT	Mix id	Beam dimensions (mm)	Longitudinal steel	steel ratio μ (%)	Span L_0 (mm)
1	M1	150 × 200 × 2200	2Æ12	0.97	2000
2	M2	150 × 200 × 2200	2Æ12	0.97	2000
3	M3	150 × 200 × 2200	2Æ12	0.97	2000

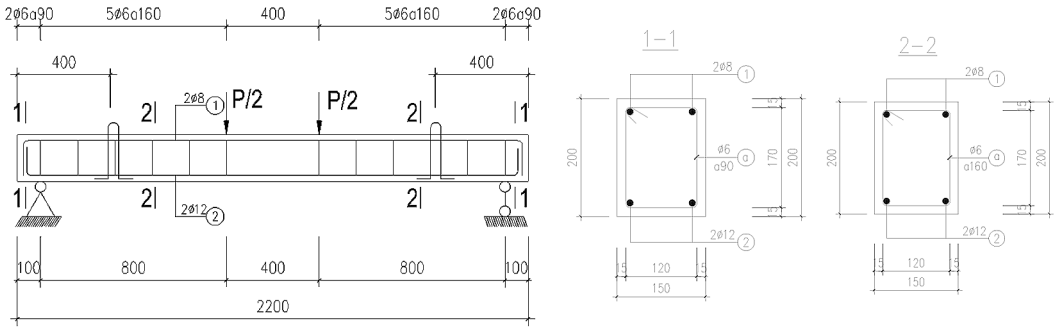

(a) Beam configuration **(b) Beam cross-section**

Figure 5. Four-point bending test setup and instrumentation layout

RESULTS

Mechanical properties

The results of the mechanical properties experiments of RLWAC are shown in Table 4 and Figure 6.

The experimental results show that the mechanical properties of RLWAC vary consistently with strength level, with three groups exhibiting characteristic compressive strengths of approximately 15 MPa (M1), 21–22 MPa (M2), and 30–31 MPa (M3). The corresponding measured splitting tensile strengths range from approximately 1.68–1.73 MPa (M1), 2.05–2.08 MPa (M2), and 2.48–2.53 MPa (M3). Based on the experimental data, the authors propose a relationship between the splitting tensile strength and the compressive strength of RLWAC, as given in Equation 1 [27]:

Table 3. Properties of the reinforcing bars used

No	Diameter and Class of steel	As, cm²	f_y, MPa	f_u, MPa	$E_s .10^{-3}$,MPa
1	Ø12 CB400V	2.26	440	552.6	210
2	Ø8 CB400V	1.01	440	552.6	210
3	Ø6 CB240T	0.566	240.2	305.5	210

Table 4. Mechanical and physical properties of recycled lightweight aggregate concrete

No.	Mix id	The age of hardening, day	Compressive strength f_c, MPa	Splitting tensile strength, $f_{ct,sp}$ MPa	Flexural tensile strength, f_r , MPa	Elastic modulus, E_c, MPa
1	M1	28 days	15.11	1.73	2.91	12903
2	M2	28 days	21.11	2.07	3.54	15591
3	M3	28 days	30.68	2.48	4.17	17967

$$f_{ct,sp} = 0.50.\sqrt{\frac{\rho_c}{2200}}\sqrt{f_c}\ [\text{MPa}] \quad (1)$$

where: $f_{ct,sp}$,f_c denote the splitting tensile strength [MPa] and the compressive strength [MPa] of RLWAC, respectively.

The relationship between flexural tensile strength and the splitting tensile strength of RLWAC is given by Equation 2:

$$f_r = \gamma . f_{ct,sp} \approx 1.67 f_{ct,sp}\ [MPa] \quad (2)$$

where: γ is the ratio between the flexural tensile strength and the splitting tensile strength, with $\gamma = f_r/f_{ct,sp}$. According to published research results [27], the value of γ ≈1.67.

The elastic modulus of RLWAC was determined from compression test results in accordance with ASTM C469 [25]. The relationship between the elastic modulus, the compressive strength, and the bulk density of RLWAC is proposed as given in Equation 3 [27]:

$$E_c = 19520\left(\frac{f_c}{10}\right)^{0,3} (\rho/2200)^2\ [\text{MPa}] \quad (3)$$

where: E_c, ρ_c, f_c denote the elastic modulus (MPa), the bulk density (kg/m³), and the compressive strength (MPa) of RLWAC, respectively.

Equations 1, 2, and 3 are used as material inputs for subsequent analyses of the bond-slip behavior and the mechanisms of crack initiation and propagation in reinforced concrete beams using RLWAC

The experimental results for the stress-strain relationship of RLWAC for mixes M1, M2, and M3 are shown in Figure 6 [27].

The stress-strain curves of specimens within the same strength grade exhibit good consistency. The behavior of RLWAC can be divided into two main stages: in the initial stage, the stress-strain curve of the concrete is nearly linear. When the stress reaches approximately 85% of the peak strength, the stress-strain curve of the concrete gradually transitions to a nonlinear shape. After reaching the peak stress, the concrete specimens quickly fail and almost immediately lose their load-bearing capacity.

The experimental results show that the strain at the peak stress of RLWAC is $e_{c1} \approx 0.0028$. The ultimate strain at complete failure, $e_{cu1,}$ was recorded to be very close to e_{c1}, reflecting the high brittleness and the limited post-peak deformation capacity of RLWAC. Due to the difficulty in accurately determining e_{cu2} under the experimental

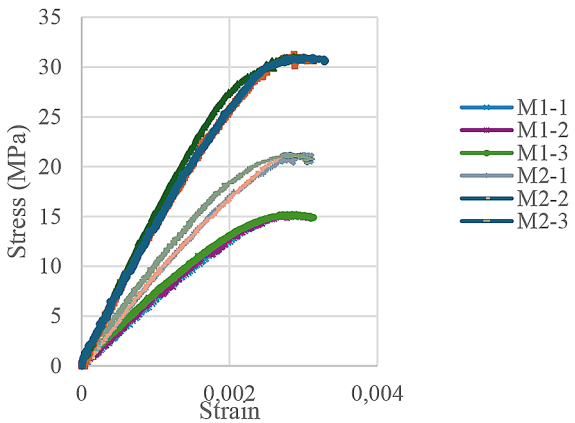

Figure 6. Stress–strain curves of RLWAC for specimen groups M1, M2, and M3

conditions, the ultimate strain was taken by reference to EN 1992-1-1[14] for lightweight concrete, with e_{cu2} = 0.0031within the density range of the studied lightweight concrete. Therefore, the authors propose that the stress-strain relationship of RLWAC be approximated by a single linear segment, with the ultimate strain $e_{cu2} \approx$ 0.0031. This proposed stress-strain model is used in subsequent analyses of flexural behavior and the mechanisms of crack initiation and propagation in reinforced concrete beams using RLWAC.

Bond characteristics

The relationship between bond stress and slip of reinforcing steel in RLWAC was determined through pull-out tests conducted on specimens from three mix designs, M1, M2, and M3, as shown in Figure 7 [27].

In stage I, when the slip is very small (s ≈ 0), the concrete remains uncracked, and the bond-slip relationship between the reinforcement and the concrete is linear. According to the results reported by [29], [30] and [31], in this stage, the bond stress is mainly transferred through chemical bonding between the surface of the reinforcement and the cement paste in the reinforcement-concrete interfacial transition zone (ITZ).

In Stage II, the bond-slip relationship curve takes a nonlinear form, with the bond stress increasing. According to [30] and [31], at this stage, cracks appear in the concrete around the reinforcement. Because the chemical bonding is reduced, the mechanical interlocking mechanism due to the ribs of the reinforcing bar bearing against and "biting into" the surrounding concrete becomes dominant. The bond stress approaches the value τ_{max}, and at the same time, the slip of the reinforcing bar relative to the concrete begins to increase, but at a very slow rate.

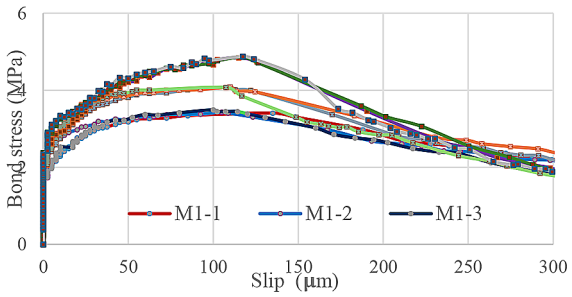

Figure 7. Bond–slip curves of concrete up to complete pull-out failure for the three RLWAC mix groups M1, M2, and M3

In stage III, after reaching its maximum value, the bond stress remains nearly constant for a very short period before starting to decrease. As slip increases, the bond stress decreases toward the corresponding value τ_f . According to research [31], in this stage, the concrete in front of the ribs of the reinforcing bar is crushed and locally damaged, gradually reducing the effectiveness of the mechanical interlocking mechanism. As a result, the bond stress decreases with slip in the range from s_1 to s_2. In this stage, contact friction between the reinforcement and the concrete begins to play an increasingly significant role. For concrete using lightweight aggregates, according to [30], [31], the effectiveness of friction and mechanical interlocking is lower than that of normal-weight concrete. This is explained by the fact that lightweight aggregates have low hardness and compressive strength, the ITZ is weak and easily forms microcracking, and the bond stress decreases rapidly after the maximum point in the bond-slip curve, reflecting the high brittleness of the material.

In stage IV, the bond stress is considered to remain constant until the steel bar is pulled out of the concrete. This can be explained as follows: when the slip is greater than s_2, the mechanical interlocking mechanism is almost ineffective, the remaining bond resistance is mainly due to the residual friction between the steel and the damaged concrete, with the bond stress approximately equal to the value τ_f and nearly constant with increasing the slip [30], [31].

Based on the integration of the τ–s curve over the anchorage length of 5d, the formula for determining the average bond stress of RLWAC is given by Equation 4 [27]:

$$\bar{\tau} = 1.60\sqrt{\frac{2200}{\rho_c}} f_{ct} \text{ [MPa]} \qquad (4)$$

Where, according to research [19]: f_{ct} = 0.9 $f_{ct,sp}$; For RLWAC, the following proposed formula [27] is used: $f_{ct,sp} = 0.50.\sqrt{\frac{\rho_c}{2200}}\sqrt{f_c}$ [Mpa]

The experimental research results and comparison with commonly used predictions for lightweight concrete, show that: at the same compressive strength level, the average bond stress $\bar{\tau}$ of RLWAC is smaller than the values predicted by K.H. Mo [32], E. Sancak [33], but is close to those predicted by CEB - FIP [34] and W.C. Tang [14] (Figure 8).

It can be seen that the bond stress transfer mechanism in RLWAC is similar to that of normal-weight concrete, including chemical bonding, mechanical interlocking, and contact friction. Compared with previous research results, the average bond stress value of RLWAC is generally lower than that of conventional lightweight and normal-weight concrete. According to studies [35], [36], and [30], this is due to the lower density and elastic modulus of the concrete, as well as significantly weakened mechanical interlocking and friction effects.

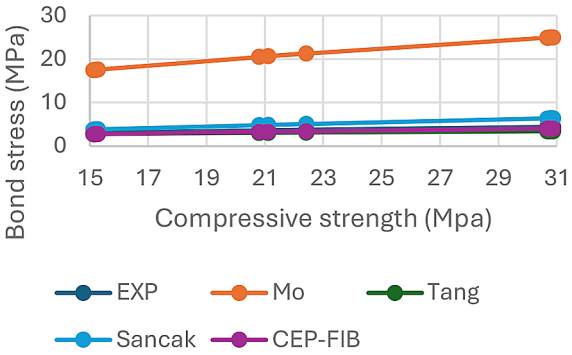

Figure 8. Average bond strength of RLWAC compared with prediction models

Results on crack formation and development

Experimental results on crack formation and development of RLWAC beams under flexural loading are shown in Figure 9, Figure 10.

The research results showed that, under loading, cracks appeared earlier in RLWAC beams than in normal-weight concrete (BTT) beams. After crack initiation, the crack width of RLWAC beams was greater than that of BTT beams at the same load level.

This can be explained by the mechanical characteristics of RLWAC and the bond behavior between the steel reinforcement and the concrete.

Firstly, the bond strength between the steel reinforcement and RLWAC is significantly lower than that of normal-weight concrete. This issue is discussed in section 3.2 of this study. This finding is also consistent with the results of the publication [30].

Secondly, the tensile strength of RLWAC is lower than that of conventional reinforced concrete. RLWAC exhibits brittle behavior, leading to early cracking and localized failure.

The load–reinforcement strain relationships of RLWAC for specimen groups M1, M2, and M3 indicate that the reinforcement strains in the beams evolve similarly when the load increases, and a comparison with the M3 sample of normal-weight concrete having the same compressive strength is presented in Figure 11.

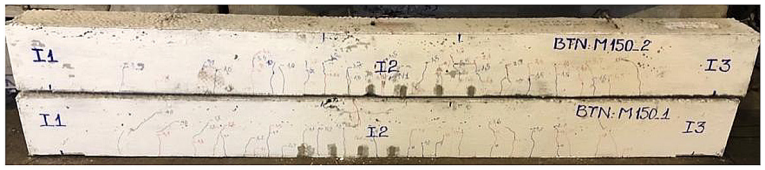

(a) Cracks observed in the beam specimen with concrete mix M1

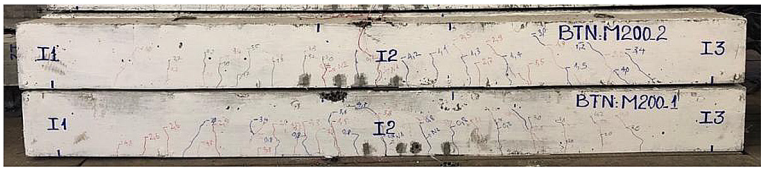

(b) Cracks observed in the beam specimen with concrete mix M2

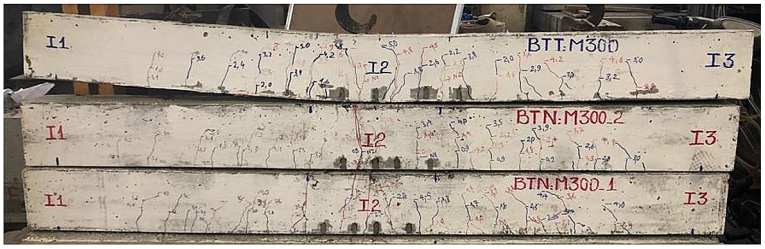

(c) Cracks observed in the beam specimen with concrete mix M3 and normal-weight concrete (BTT)

Figure 9. Images of cracks in the experimental beams

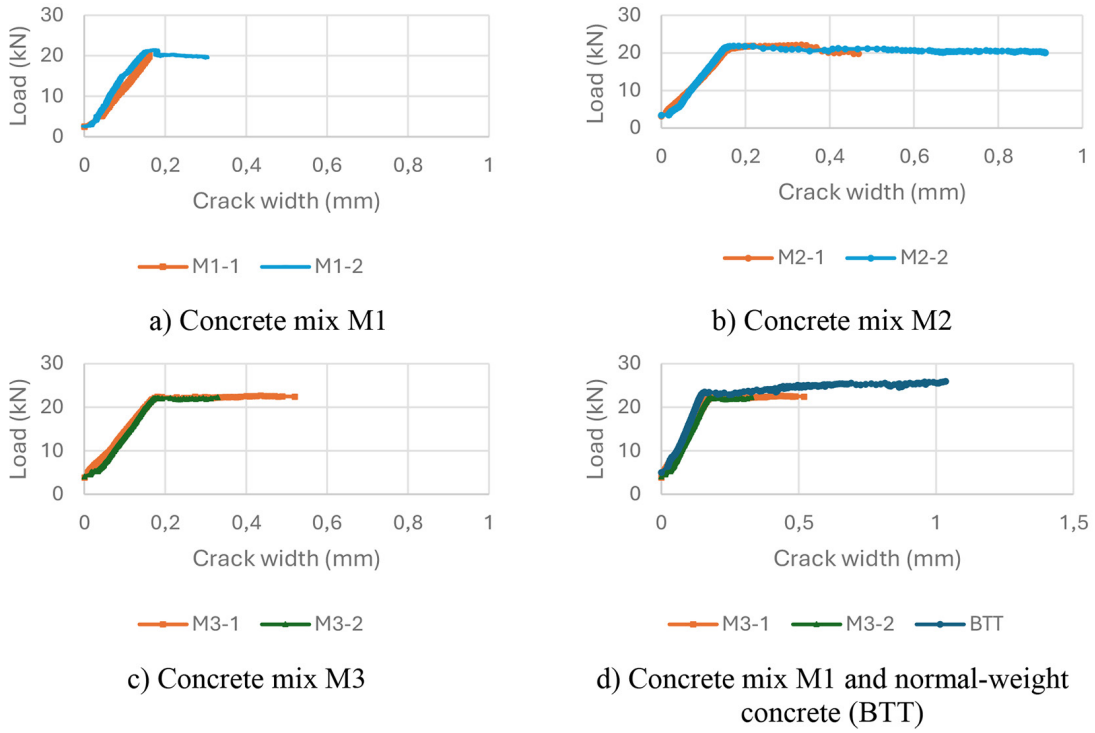

Figure 10. Load–crack width relationships of the test beams for specimen groups M1, M2, and M3

The load-strain curves of the reinforcement in the RLWAC and normal-weight concrete beams show that, in the elastic stage, the steel strain in both RLWAC and BTT beams is almost equivalent. However, as soon as the reinforcement begins to yield, the RLWAC specimens exhibit a faster rate of increase in strain due to the reduced force transfer efficiency after cracking initiation and the gradually decreasing bond stress. At the same time, the compression zone strain of the RLWAC in specimens M1, M2, and M3 shown in Figure 12 as shows similar values at the same load level; however, Figure 12 also indicates that the compression zone strain of the RLWAC is significantly larger than that of the normal-weight concrete with the same compressive strength at the same load level. This reflects the characteristics of RLWAC, which has a low elastic modulus and a porous RLWA structure with crushing strength, leading to greater compressive deformation under the same load. This results in faster concrete deformation in the tension zone and accelerated crack widening.

Thus, it can be seen that, due to the low bond stress, low tensile strength, low elastic modulus, and the rapid increase in steel strain after yielding, RLWAC exhibits earlier crack initiation, faster crack development, and larger crack width compared to normal-weight concrete (BTT).

Model for predicting crack initiation and propagation

In the pre-cracking stage, the calculation model is based on the following assumptions:

1. The plane section remains plane.
2. The concrete in the compression zone behaves elastically, with a triangular stress distribution.
3. RLWAC exhibits brittle behavior, and the tensile zone is assumed to remain linear up to cracking (triangular stress diagram).
4. The reinforcement behaves elastically and is strain-compatible with the concrete.
5. The reinforcement area is transformed into an equivalent concrete area using the coefficient: $\alpha_e = \frac{E_s}{E_c}$. At the moment when the beam starts to crack, the extreme tensile stress of the concrete reaches the axial tensile strength f_{ct}.

The crack moment of the beam is determined according to [19]:

$$M_{crc} = f_s A_s \left(d - \frac{x}{3}\right) + \\ + \frac{f_{ct}(h-x)hb}{3} \tag{5}$$

where: f_s *denotes* the stress in the reinforcement at the time of cracking.

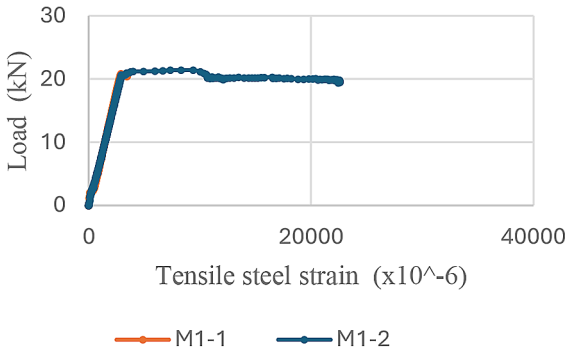

a) Concrete mix M1

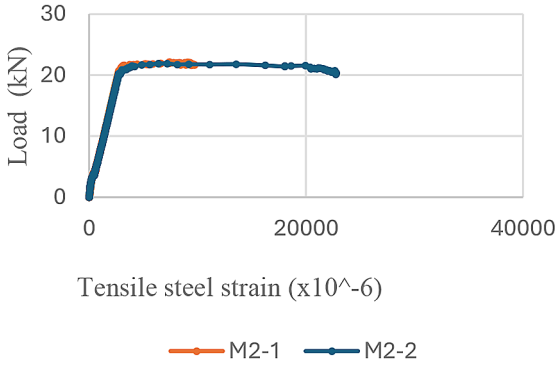

b) Concrete mix M2

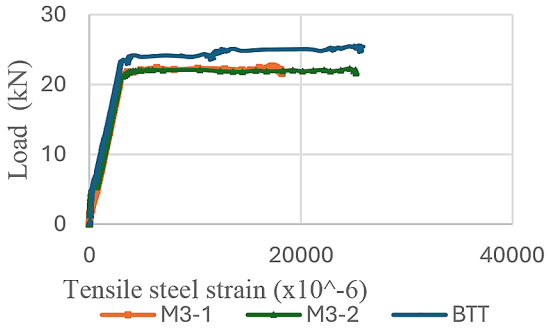

c) Concrete mix M3 and normal-weight concrete (BTT)

Figure 11. Load–strain relationships of tensile reinforcement for beam specimens M1, M2, M3, and normal-weight concrete (BTT)

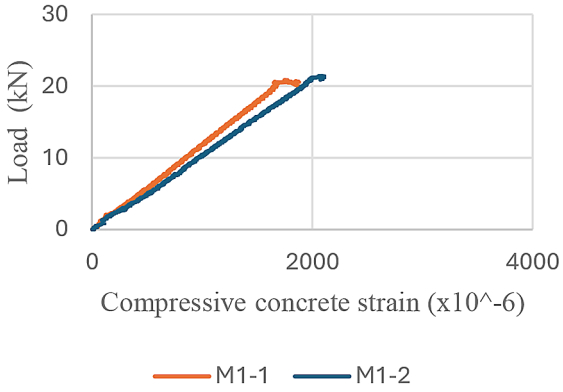

a) Concrete mix M1

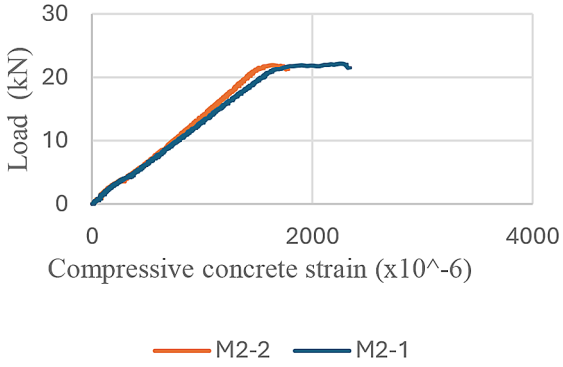

b) Concrete mix M2

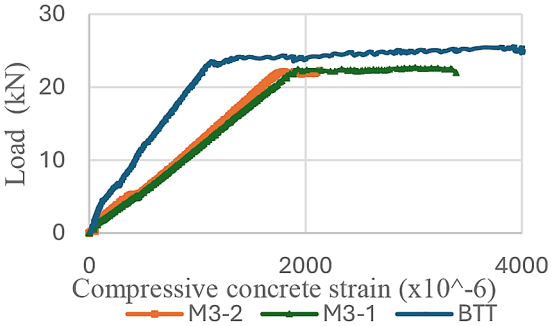

c) Concrete mix M3 and normal-weight concrete (BTT)

Figure 12. Load–strain relationships of concrete in the compression zone for beam specimens M1, M2, M3, and normal-weight concrete (BTT)

Considering the effect of tension stiffening in the region between cracks, the crack spacing, and the crack width, the following formula is proposed according to [34]:

$$l_{crc} = \frac{f_{ct} A_{ct,ef}\, D}{2\bar{\tau} A_s} \tag{6}$$

When expressed in terms of moment, by substituting σ_s from the moment-stress relationship of the reinforcement into the above formula, the crack width can be written as:

$$w = \frac{l_{crc}}{E_s}\left(\frac{3M}{A_s d(3-\beta)} - \bar{\tau}\frac{l_{crc}}{D}\right) \tag{7}$$

In this case, $\bar{\tau}$ is the average bond stress. For RLWAC, it is recommended to use the following published formula [27]:

$$\bar{\tau} = 1.60\sqrt{\frac{2200}{\rho_c}} f_{ct}\ [\text{MPa}] \tag{8}$$

In which, according to [19]: $f_{ct} = 0.9f_{ct,sp}$; For RLWAC, the following proposed formula [27] is used:

$$f_{ct,sp} = 0.50.\sqrt{\frac{\rho_c}{2200}}\sqrt{f_c}\ [\text{Mpa}] \qquad (9)$$

COMPARISON OF EXPERIMENTAL RESULTS AND THEORETICAL MODEL

The calculated cracking moment values obtained from the proposed theoretical model and the experimental results are presented in Table 5.

The crack formation moment, Mcrc, determined by the model is in close agreement with the experimental results, with an error of only 2% to 7% for all three mix designs, M1, M2, and M3. This indicates that the proposed model accurately reflects the crack formation mechanism of RLWAC beams.

The Mcrc value determined according to TCVN 5574:2018 [18] is higher than the experimental results by 11% to 31%, while the prediction according to EC2 [19] is lower by 10% to 23%. These discrepancies indicate that both current standards do not accurately describe the cracking behavior of RLWAC, which exhibits

Table 5. M_{crc} of the studied RLWAC beams

Mix id	M_{crc} (experimental) (kN.m)	M_{crc} (theoretical) (kN.m)	Difference	M_{crc} TCVN -5574 (kN.m)	Difference	M_{crc} EC2 (kN.m)	Difference
M1	2.02	2.16	7%	2.64	31%	1.56	-23%
M2	2.64	2.72	3%	3.06	16%	2.30	-13%
M3	3.22	3.28	2%	3.57	11%	2.90	-10%

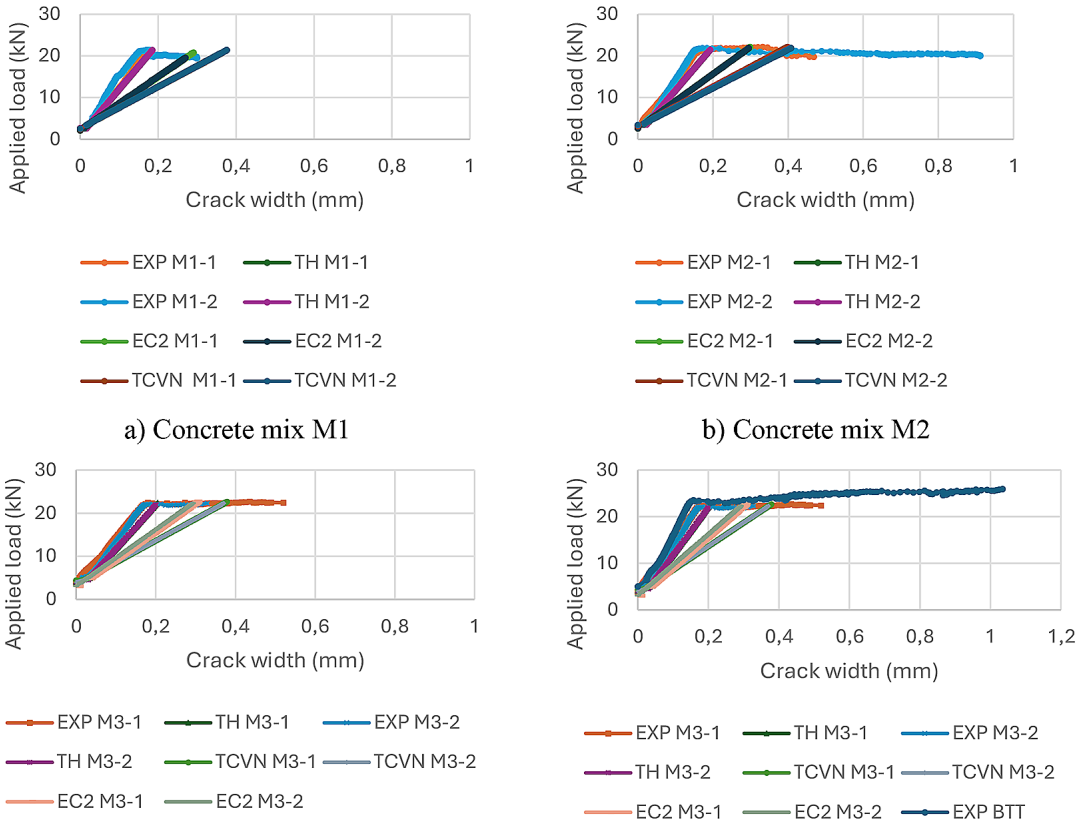

a) Concrete mix M1

b) Concrete mix M2

c) Concrete mix M3

d) Concrete mix M3 and normal-weight concrete (BTT)

Figure 13. Load–crack width relationship of RLWAC based on experimental results, proposed theoretical calculations, and design codes (TCVN 5574:2018 and EC2)

Table 6. Crack width at the steel yielding stage based on experimental results, theoretical calculations, and TCVN 5574:2018

P (kN)	ID mix	W_{crc} (experimental-EXP) (mm)	W_{crc} (theoretical-TH) (mm)	Difference	W_{crc} (EC2) (mm)	Difference	W_{crc} (TCVN 5574:2018) (mm)	Difference
18.79	M1-1	0.133	0.161	21%	0.257	93%	0.324	144%
18.89	M1-2	0.132	0.162	23%	0.259	96%	0.326	147%
19.89	M2-1	0.148	0.177	20%	0.264	78%	0.340	130%
19.04	M2-2	0.151	0.179	19%	0.262	74%	0.345	128%
20.74	M3-1	0.158	0.188	19%	0.268	70%	0.348	120%
20.44	M3-2	0.156	0.185	19%	0.265	70%	0.350	124%

mechanical properties different from those of normal-weight concrete.

The results of determining the crack width at the time of plastic yielding of the reinforcement according to TCVN5574:2018 [18], Eurocode 2 [19], and experimental results are presented in Table 6 and Figure 13. The calculated value from the proposed l model is consistent with the experimental results, with an error of 19–23%. The calculation results reasonably accurately simulates the observed crack size in the experiment. Meanwhile, the calculated crack width according to TCVN 5574:2018 [18] is 120% to 147% higher than the experimental results. The calculated crack width according to Eurocode 2 [19] is also larger than the experimental results by 70% to 93%, and both standards are overly cautious and do not accurately reflect the characteristics of RLWAC. Therefore, the results indicate that the proposed model for calculating the cracking moment and crack width of RLWAC beams yields predictions that are more consistent with the actual behavior of RLWAC than those provided by the formulas specified in TCVN 5574:2018 [18] and Eurocode 2 [19].

CONCLUSIONS

Based on the experimental results and analysis of reinforced concrete beams using RLWAC, the following conclusions can be drawn:

- The mechanical properties of RLWAC are greatly influenced by the porous nature, high water absorption, and low crushing strength of the RLWA. The elastic modulus and tensile strength of RLWAC are lower than those of normal-weight concrete. Therefore, when RLWAC beams are subjected to flexural loading, earlier crack initiation occurs, and larger crack widths are compared to those of normal-weight concrete beams. Based on experimental research results, this study proposes a predictive model for the tensile strength and elastic modulus of reinforced concrete using RLWAC.
- The bond-slip behavior of RLWAC shows that the force transmission mechanism and the development stages in the bond stress-slip relationship still go through 4 stages, like normal-weight concrete, but the maximum bond stress value is lower. The ITZ region of RLWAC is weak, prone to microcracking, which reduces the effectiveness of the mechanical interlocking mechanism and significantly reduces friction. The study has developed a τ–s model with three segments and proposed a suitable formula for calculating the average bond stress for RLWAC, helping to more accurately describe the force transmission mechanism between concrete and reinforcement.
- Flexural tests on beams showed a direct influence of bond stress on the crack mechanism initiation and propagation mechanisms. RLWAC beams showed earlier crack initiation, greater number of cracks, and a crack propagation rate compared to BTT beams. This is due to the low bond stress, low tensile strength, and low elastic modulus of RLWAC.
- This study proposes a theoretical model to predict the crack initiation and propagation in flexural reinforced concrete beams using RLWAC, which has a relatively good agreement with experimental results. The crack resistance moment, M_{crc}, was predicted by the proposed model and compared with the experimental results, with an error of about 2–7%. The crack width at the time of yielding steel was predicted by the proposed model and compared with the experimental results,

with an error of about 19–23%. Meanwhile, the predictions according to TCVN 5574:2018 and Eurocode 2 are overly conservative with errors of about 70– 147%.

This research provides an important basis for developing appropriate design and crack control criteria for RLWAC structural elements in the future.

REFERENCES

1. Xiao J., Zhang K., Zhang Q. Strain rate effect on compressive stress–strain curves of recycled aggregate concrete with seawater and sea sand. Construction and Building Materials. 2021; 300: 124014. https://doi.org/10.1016/j.conbuildmat.2021.124014
2. Masud M., Dhaka B., Abdisamad A,. Omar., Supervisor., Ali Omar A. Comparative study on compressive strength of demolished concrete aggregate and conventional concrete aggregate for construction. 2022.
3. Vázquez E. Recycled aggregates for concrete: Problems and possible solutions. International Journal of Earth & Environmental Sciences. 2016; 1:122. https://doi.org/10.15344/2456-351X/2016/122
4. Luo H., Aguiar J., Wan X., Wang Y., Cunha S., Jia Z. Application of Aggregates from construction and demolition wastes in concrete: Review. Sustainability. 2024; 16(10): 4277. https://doi.org/10.3390/su16104277
5. Luo S., Ye S., Xiao J., Zheng J., Zhu Y. Carbonated recycled coarse aggregate and uniaxial compressive stress-strain relation of recycled aggregate concrete. Construction and Building Materials. 2018; 188: 956–65. https://doi.org/10.1016/j.conbuildmat.2018.08.159
6. Chang YC., Wang YY., Zhang H., Chen J., Geng Y. Different influence of replacement ratio of recycled aggregate on uniaxial stress-strain relationship for recycled concrete with different concrete strengths. Structures. 2022; 42:284–308. https://doi.org/10.1016/j.istruc.2022.05.117
7. Reis GS dos., Quattrone M., Ambrós WM., Grigore Cazacliu B., Hoffmann Sampaio C. Current applications of recycled aggregates from construction and demolition: A review. Materials. 2021; 14(7): 1700. https://doi.org/10.3390/ma14071700
8. Pacheco J., de Brito J. Recycled aggregates produced from construction and demolition waste for structural concrete: Constituents, properties and production. Materials. 2021; 14(19): 5748. https://doi.org/10.3390/ma14195748
9. Silva RV., de Brito J., Dhir RK. Properties and composition of recycled aggregates from construction and demolition waste suitable for concrete production. Construction and Building Materials. 2014; 65: 201–17. https://doi.org/10.1016/j.conbuildmat.2014.04.117
10. McNeil K., Kang T. Recycled concrete aggregates: A review. International Journal of Concrete Structures and Materials. 2013; 7. https://doi.org/10.1007/s40069-013-0032-5
11. Arezoumandi M., Steele AR., Volz JS. Evaluation of the bond strengths between concrete and reinforcement as a function of recycled concrete aggregate replacement level. Structures. 2018; 16: 73–81. https://doi.org/10.1016/j.istruc.2018.08.012
12. Yang H., Huang Y., Lv L. Bond behavior between recycled aggregate concrete and steel rebar subjected to biaxial lateral pressure. Structures. 2022; 41: 139–46. https://doi.org/10.1016/j.istruc.2022.04.085
13. Xiao, J. Recycled aggregate concrete structures. Springerprofessional. 2018.
14. Tang WC., Lo TY., Balendran RV. Bond performance of polystyrene aggregate concrete (PAC) reinforced with glass-fibre-reinforced polymer (GFRP) bars. Building and Environment. 2008; 43(1): 98–107. https://doi:10.1016/j.buildenv.2006.11.030
15. Anwar Hossain KM. Bond characteristics of plain and deformed bars in lightweight pumice concrete. Construction and Building Materials. 2008; 22(7): 1491–9. https://doi:10.1016/j.conbuildmat.2007.03.025
16. Su T., Wang C., Cao F., Zou Z., Wang C., Wang J., et al. An overview of bond behavior of recycled coarse aggregate concrete with steel bar. Reviews on Advanced Materials Science. 2021; 60(1): 127–44. https://doi.org/10.1515/rams-2021-0018
17. Zhu Q., Chen J., He Y., Sun X. Bond stress distribution and bond–slip model of deformed steel bars in iron tailing sand recycled aggregate concrete. Buildings. 2023; 13(5): 1176. https://doi.org/10.3390/buildings13051176
18. TCVN 5574:2018. Design of concrete and reinforced concrete structures. 2018.
19. EN 1992-1-1, Eurocode 2. Design of Concrete Structures – Part 1-1: General Rules and Rules for Buildings. 2004.
20. Mueller A., Sokolova SN., Vereshagin VI. Characteristics of lightweight aggregates from primary and recycled raw materials. Construction and Building Materials. 2008; 22(4): 703–12. https://doi:10.1016/j.conbuildmat.2007.06.009
21. TCVN 7572:2006. Aggregates for concrete and mortar – Test methods. 2006.
22. TCVN 3118:2022. Heavy concrete – Method for determination of compressive strength. 2022.
23. TCVN 3119:2022. Heavy concrete – Method for determination of tensile strength. 2022.

24. TCVN 8862:2011. Standard test method for splitting tensile strength of cement-bound granular materials. 2011.
25. ASTM C469-94. Standard Test Method for Static Modulus of Elasticity and Poisson's Ratio of Concrete in Compression. ASTM International; 1994.
26. SNIP 2.03.01-84. Concrete and Reinforced Concrete Structures – Design Code for Heavyweight and Lightweight Concrete. 1984.
27. Nguyen H.P., Le N.L., Nguyen T.-T.T., Nguyen C.T., and Nguyen V.T. Mechanical properties of structural lightweight concrete using lightweight aggregates from construction and demolition waste. International Journal of Geomate. 2023; 25(110): 40–48. https://doi.org/10.21660/2023.110.3921
28. Zhang M.H., Gjorv O.E. Mechanical properties of high-strength lightweight concrete. ACI Materials Journal 1991; 88(3). https://doi.org/10.14359/1839
29. Yang X., Wu T., Liu X., Liu Y. Bond-slip relationship of rebar in lightweight aggregate concrete. Structures. 2022; 45: 2198–209. https://doi.org/10.1016/j.istruc.2022.10.010
30. Lundgren K. Three-Dimensional Modelling of Bond in Reinforced Concrete. PhD Thesis, 1999.
31. Alexandre Bogas J., Gomes MG., Real S. Bonding of steel reinforcement in structural expanded clay lightweight aggregate concrete: The influence of failure mechanism and concrete composition. Construction and Building Materials. 2014; 65: 350–9. http://dx.doi.org/10.1016/j.conbuildmat.2014.04.122
32. Mo KH., Alengaram UJ., Visintin P., Goh SH., Jumaat MZ. Influence of lightweight aggregate on the bond properties of concrete with various strength grades. Construction and Building Materials. 2015; 84: 377–86. http://dx.doi.org/10.1016/j.conbuildmat.2015.03.040
33. Sancak E. Prediction of bond strength of lightweight concretes by using artificial neural networks. Scientific Research and Essays. 2009. 4(4): 256–266.
34. CEB-FIB. Model Code for Concrete Structures. 2013.
35. Kaffetzakis MI., Papanicolaou CG. Bond behavior of reinforcement in lightweight aggregate self-compacting concrete. Construction and Building Materials. 2016; 113: 641–52. http://dx.doi.org/10.1016/j.conbuildmat.2016.03.081
36. Abed MA., Alkurdi Z., Fořt J., Černý R., Solyom S. Bond behavior of FRP bars in lightweight SCC under direct pull-out conditions: Experimental and numerical investigation. Materials (Basel). 2022; 15(10): 3555. https://doi.org/ma15103555 PubMed PMID: 35629582; PubMed Central PMCID: PMC9145959